



ELSEVIER

Nuclear Physics A682 (2001) 22c–27c

[www.elsevier.nl/locate/npe](http://www.elsevier.nl/locate/npe)

## Measurement and analysis of quadruple ( $\alpha\gamma\gamma$ ) angular correlations for high spin states of $^{24}\text{Mg}^*$

I. Wiedenhöver<sup>a,†</sup>, A.H. Wuosmaa<sup>a</sup>, C.J. Lister<sup>a</sup>, M.P. Carpenter<sup>a</sup>, R.V.F. Janssens<sup>a</sup>, H. Amro<sup>a,‡</sup>, J. Caggiano<sup>a</sup>, A. Heinz<sup>a</sup>, F.G. Kondev<sup>a</sup>, T. Lauritsen<sup>a</sup>, S. Siem<sup>a,§</sup>, A. Sonzogni<sup>a</sup>, P. Bhattacharyya<sup>b</sup>, M. Devlin<sup>c,¶</sup>, D.G. Sarantites<sup>c</sup>, L.G. Sobotka<sup>c</sup>

<sup>a</sup>Argonne National Laboratory, Argonne, Illinois 60439, USA

<sup>b</sup>Purdue University, West Lafayette, Indiana 47907, USA

<sup>c</sup>Dept. of Chemistry, Washington University, St. Louis, Missouri 63130, USA

The high-lying,  $\alpha$ -decaying states in  $^{24}\text{Mg}$  have been studied by measuring the complete decay path of  $\alpha$  and  $\gamma$  emissions using five segmented Silicon detectors in conjunction with GAMMASPHERE. We analyzed the ( $\alpha\gamma$ ) triple angular correlations and, for the first time, ( $\alpha\gamma\gamma$ ) quadruple correlations. The data analysis is based on a new Fourier transformation technique. The power of the technique is demonstrated.

### 1. INTRODUCTION

The interest in high spin states of  $^{24}\text{Mg}$  is based, at least in part, in the special position that this nucleus occupies on the nuclear chart. It is heavy enough to show a strong deformation and, at the same time, sufficiently light to be calculated with the shell model. The search for high spin states approaching spin 12, the terminating spin within the sd-shell, has been the subject of many experimental investigation, e.g. [1–4]. In most cases, the experiments measured the population of these states and reaction models of the Hauser-Feshbach type were used to assign spins, see e.g. [1,2]. The spin assignments from those studies depend on the adjustment of parameters and are usually reliable to within one unit. To this point, firm assignments to high spin states come from measurements of triple angular correlations between the beam axis, one  $\alpha$  particle and one  $\gamma$ -ray [3,4]. The present paper describes the first measurement of quadruple ( $\alpha\gamma\gamma$ ) angular correlations and the new data analysis techniques that were developed for it. The results of this analysis and the implications for the nuclear structure of  $^{24}\text{Mg}$  are the subject of a forthcoming publication [6].

\*Work supported by the U.S. Department of Energy, Nuclear Physics Division, under Contracts No. W-31-109-ENG-38 and DE-FG05-88ER40406.

<sup>†</sup>present address: NSCL, Michigan State University, East Lansing, Michigan 48824, USA

<sup>‡</sup>present address: Mississippi State University, Mississippi State, Mississippi 39372, USA

<sup>§</sup>present address: University of Oslo, Oslo, Norway

<sup>¶</sup>present address: Los Alamos National Laboratory, Los Alamos, New Mexico 87545, USA

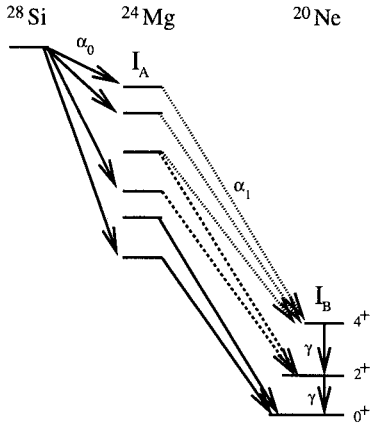


Figure 1. schematic decay path of the  $\alpha$  and  $\gamma$  radiation.

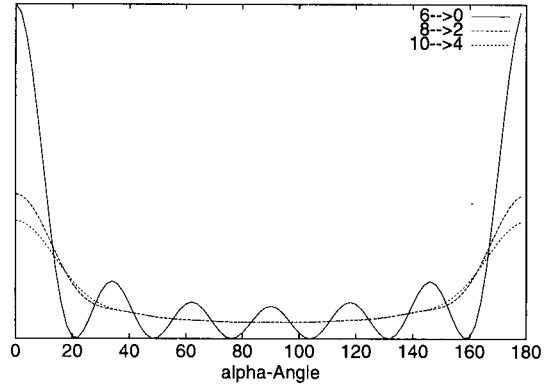


Figure 2. Calculated angular distributions for  $\alpha_1$  radiation emitted from  $^{24}\text{Mg}$  excited states. The distributions feeding the  $^{20}\text{Ne}$  ground state, the  $2^+$  and  $4^+$  states are displayed, each for  $L(\alpha) = 6$ .

## 2. EXPERIMENT

To identify the spins of the  $I \geq 8$  candidate states, we performed an experiment with the ATLAS accelerator at Argonne National Laboratory. A compact setup of five Doubly Segmented Silicon Strip Detectors (DSSD) was developed for the target chamber of GAMMASPHERE. During this experiment, the  $4\pi$  detector array GAMMASPHERE [7] was equipped with 100 escape-suppressed Germanium detectors. The states of  $^{24}\text{Mg}$  were populated in the  $^{12}\text{C}(^{16}\text{O}, \alpha)^{24}\text{Mg}$  reaction. The high-lying states decay subsequently by  $\alpha$ -emission to either the  $0^+$ ,  $2^+$  or  $4^+$  state of  $^{20}\text{Ne}$ . A sketch of the relevant decay paths is displayed in Figure 1. The  $\alpha$  particle emitted from compound states of  $^{28}\text{Si}$ , denoted as  $\alpha_0$ , was detected upstream of the target in an annular DSSD. The  $\alpha$  particles populating the  $^{20}\text{Ne}$  states, denoted as  $\alpha_1$ , were detected around  $\theta_{lab} = 45^\circ$  in four planar DSSD.

Calculated angular distributions of the  $\alpha_1$  particles are displayed in figure 2. The distributions are calculated for  $^{24}\text{Mg}$  states in the magnetic sub-state  $m = 0$ , which is a reasonable approximation for our experiment (see Sect. 3). In the case where  $\alpha_1$  feeds the  $^{20}\text{Ne}$  ground state, the angular distributions are the squared Legendre Polynomials  $P_l(\cos(\theta_{\alpha_1}))^2$ . If the excited  $2^+$  or  $4^+$  states of  $^{20}\text{Ne}$  are populated, the  $\alpha_1$  angular distributions lose their characteristic form. This is due to the fact that the final  $^{20}\text{Ne}$  state contains an incoherent superposition of several m-substates, washing out the characteristic oscillations. Since the decay towards the excited states in  $^{20}\text{Ne}$  takes over very rapidly above 15 MeV excitation, the method is limited to relatively low-lying states.

It was demonstrated [3,4] that this obstacle can be overcome for the decays feeding the  $2^+$  level, by detecting the subsequent  $^{20}\text{Ne}$   $\gamma$ -ray. By observing the complete decay path, one imposes a coherent relation between the m-substates of the  $2^+$  state in  $^{20}\text{Ne}$  and this

feature re-establishes the characteristic oscillation pattern in the  $\alpha_1$  angular distributions. Most firm spin assignments to high-lying states in  $^{24}\text{Mg}$  stem from measurements of this type [3–5], but are limited to states which show a strong decay path to the  $^{20}\text{Ne } 2^+$  state. To extend the above mentioned method towards decays involving the  $4^+$  state, one has to detect both  $\gamma$  rays in the  $4^+ \rightarrow 2^+ \rightarrow 0^+$  cascade in coincidence with the  $\alpha$ -particle: This is the aim of the present work.

The requirement of a high coincidence efficiency for the  $\alpha\gamma\gamma$ -cascades makes this experiment possible only in conjunction with a  $4\pi$ - $\gamma$  detector array, such as GAMMASPHERE. The necessity to cover the full solid angle with detectors also leads to a much more complicated data analysis. While the classic experiments [3,4] used two NaI- detectors at fixed angles, here one has to find a way to take all available angles into account and, thus, analyze five-dimensional correlation patterns. Our data analysis method, which is applied to the triple- as well as to the quadruple correlations, is based on a Fourier transformation with respect to an orthogonal basis of the correlation patterns. The technique is a generalization of a method called SpeeDCO which was used to analyze  $\gamma\gamma$ -DCO patterns measured with  $4\pi$ -detector arrays [9].

### 3. THE “DYNAMIC” ALIGNMENT AXIS

Before we develop the formalism and analysis method for the quadruple correlations, we have to discuss the influence of the compound-emitted  $\alpha_0$  particle on the correlation patterns of subsequent radiations. The ideal experiment would detect  $\alpha_0$  on the beam axis, which would transfer the  $m = 0$  sub-state of the compound nucleus to the  $^{24}\text{Mg}$  level. This situation would thus produce subsequent correlation patterns *independent* of the particular angular momentum of  $\alpha_0$ .

The need to place the Silicon detectors inside the GAMMASPHERE target chamber resulted in a setup covering laboratory angles between  $158^\circ - 168^\circ$  with one annular DSSD detector. Although those angles correspond to center of mass angles smaller than  $10^\circ$  off the beam axis, they are sufficiently large to induce  $m = 1$  and  $m = 2$  components to  $^{24}\text{Mg}$  states and have to be considered in the analysis. Calculations of the effect show that we can define a dynamic alignment axis, for which  $m = 0$  is predominant, based on the angle of  $\alpha_0$ . This “tilted” alignment axis lies inside the beam- $\alpha_0$  plane at an angle, which can be approximated by the expression  $\xi \approx L_{\alpha_0}/I_{Mg}(180^\circ - \theta_0)$ . In the data analysis, all subsequent correlation angles are measured relative to this axis. Since the  $L_{\alpha_0}$  is in principle not known, the parameter was varied to produce the largest  $\alpha_1$ -distribution amplitudes. All deduced values are consistent with population from compound states of spin  $16 \pm 1$ . In none of the analyzed cases did the spin assignment depend critically on the particular choice for  $L_{\alpha_0}$ . A similar procedure had been applied in the analysis of angular correlations of breakup fragments; for a discussion see Ref. [10].

### 4. ANGULAR CORRELATIONS

We can limit our analysis to the cases where the angular momentum of the  $\alpha_1$  particle takes on the value  $L = |I_A - I_B|$ . Deviations from these stretched decays were not observed in our experiment. The  $\alpha$ - $\gamma$  angular correlations are calculated with equations (1–3), which are analogous to the expressions given in Ref. [3]. In our notation, the terms

depending on the  $\alpha$  angles were collected in  $A^{(\lambda_0 q_0)}$  (1) and the terms depending on  $\gamma$  angles were collected in  $B_2^{(\lambda_0 q_0)}$  (2). Note also that only the  $A$  term contains the spin of interest  $I_A$ . A more elaborate deduction of the correlation formulae can be found e.g. in the discussion leading to equations (12.189) and (12.204) of Ref. [8].

$$A^{(\lambda_0 q_0)}(I_A, I_B)(\theta_{\alpha 1}) \stackrel{def}{=} \sqrt{4\pi} \sum_{M_B, M'_B} (L(-M_B) I_B M_B | I_A 0)(L(-M'_B) I_B M'_B | I_A 0) \\ \times \langle I_B || L || I_A \rangle^2 (I_B M_B I_B (-M'_B) | \lambda_0 q_0) (-1)^{I_B - M'_B} \\ \times Y_L^{-M_B}(\theta_{\alpha 1}, 0) Y_L^{-M'_B}(\theta_{\alpha 1}, 0) \quad (1)$$

$$B_2^{(\lambda_0 q_0)}(\theta_\gamma, \phi_\gamma) \stackrel{def}{=} (2\lambda_0 + 1)^{-1/2} F_{\lambda_0}(E2, 2^+ \rightarrow 0^+) Y_{\lambda_0}^{q_0}(\theta_\gamma, \phi_\gamma) \quad (2)$$

$$W(I_A, 2^+)(\theta_{\alpha 1}, \theta_\gamma, \phi_\gamma) = \sum_{\substack{\lambda_0=0..4, even \\ q_0=-\lambda_0.. \lambda_0}} A^{(\lambda_0 q_0)}(I_A, 2^+)(\theta_{\alpha 1}, 0) B_2^{(\lambda_0 q_0)}(\theta_\gamma, \phi_\gamma) \quad (3)$$

In the present work, we are interested in the situation where the  $\alpha_1$  particles populate the  $4^+$  state of  $^{20}\text{Ne}$ . The formula now has to incorporate the correlations of two  $\gamma$ -rays, which makes it a function of five geometrical angles  $(\theta_{\alpha 1}, \theta_{\gamma 1}, \phi_{\gamma 1}, \theta_{\gamma 2}, \phi_{\gamma 2})$ . Again, the terms concerning the  $\alpha$ -particle and the  $\gamma\gamma$  correlations can be separated in two expressions. The definition of  $A^{(\lambda_0 q_0)}(\theta_{\alpha 1})$  (equation 1) is identical to the  $2^+$  case.

$$B_4^{(\lambda_0 q_0)}(\theta_{\gamma 1}, \phi_{\gamma 1}, \theta_{\gamma 2}, \phi_{\gamma 2}) \stackrel{def}{=} \sum_{\lambda_2 \lambda_1 q_2 q_1} (2\lambda_2 + 1)^{-1/2} F_{\lambda_0, \lambda_1}^{\lambda_2}(E2, 4^+ \rightarrow 2^+) F_{\lambda_2}(E2, 2^+ \rightarrow 0^+) \\ \times \begin{pmatrix} \lambda_2 & \lambda_1 & \lambda_0 \\ q_2 & q_1 & q_0 \end{pmatrix} Y_{\lambda_1}^{q_1}(\theta_{\gamma 1}, \phi_{\gamma 1}) Y_{\lambda_2}^{q_2}(\theta_{\gamma 2}, \phi_{\gamma 2}) \quad (4)$$

$$W(I_A, 4^+)(\theta_{\alpha 1}, \theta_{\gamma 1}, \phi_{\gamma 1}, \theta_{\gamma 2}, \phi_{\gamma 2}) = \sum_{\substack{\lambda_0=0..8, even \\ q_0=-\lambda_0.. \lambda_0}} A^{(\lambda_0, q_0)}(I_A, 4^+)(\theta_{\alpha 1}) B_4^{(\lambda_0, q_0)}(\theta_{\gamma 1}, \phi_{\gamma 1}, \theta_{\gamma 2}, \phi_{\gamma 2}) \quad (5)$$

Our new data analysis method is based on the observation that the  $B_2^{(\lambda_0, q_0)}$  and  $B_4^{(\lambda_0, q_0)}$  coefficients form an orthogonal basis of the two- or four-dimensional subspaces containing the  $\gamma$  or  $\gamma\gamma$  correlation patterns, respectively. To obtain a Fourier-transformed representation of the experimental correlations  $w_2$  and  $w_4$ , we fold them with the basis vectors  $B_2$  and  $B_4$  for a relevant set of indices  $(\lambda_0, q_0)$ .

$$s_2^{(\lambda_0, q_0)}(\theta_{\alpha 1}) = \sum_{\theta_\gamma, \phi_\gamma} w_2(\theta_{\alpha 1}, \theta_\gamma, \phi_\gamma) \frac{B_2^{(\lambda_0, q_0)}(\theta_\gamma, \phi_\gamma)}{\|B_2^{(\lambda_0, q_0)}\|} \quad (6)$$

$$s_4^{(\lambda_0, q_0)}(\theta_{\alpha 1}) = \sum_{\theta_{\gamma 1}, \phi_{\gamma 1}, \theta_{\gamma 2}, \phi_{\gamma 2}} w_4(\theta_{\alpha 1}, \theta_{\gamma 1}, \phi_{\gamma 1}, \theta_{\gamma 2}, \phi_{\gamma 2}) \frac{B_4^{(\lambda_0, q_0)}(\theta_{\gamma 1}, \phi_{\gamma 1}, \theta_{\gamma 2}, \phi_{\gamma 2})}{\|B_4^{(\lambda_0, q_0)}\|} \quad (7)$$

From the structure of equations (3) and (5) it is obvious that the Fourier-transformed representations  $s_2^{(\lambda_0, q_0)}$  and  $s_4^{(\lambda_0, q_0)}$  will be compared to the calculated  $A^{(\lambda_0, q_0)}(I_A, 2^+)(\theta_{\alpha 1})$  and  $A^{(\lambda_0, q_0)}(I_A, 4^+)(\theta_{\alpha 1})$ , respectively. Calculations of the  $A^{(\lambda_0, q_0)}(I_A, I_B)$  also show that only the terms with the maximal possible value of  $\lambda_0 = 2I_B$  show the strong oscillation patterns, i.e.  $\lambda_0 = 4$  for  $2^+$ -feeding and  $\lambda_0 = 8$  for  $4^+$ -feeding.

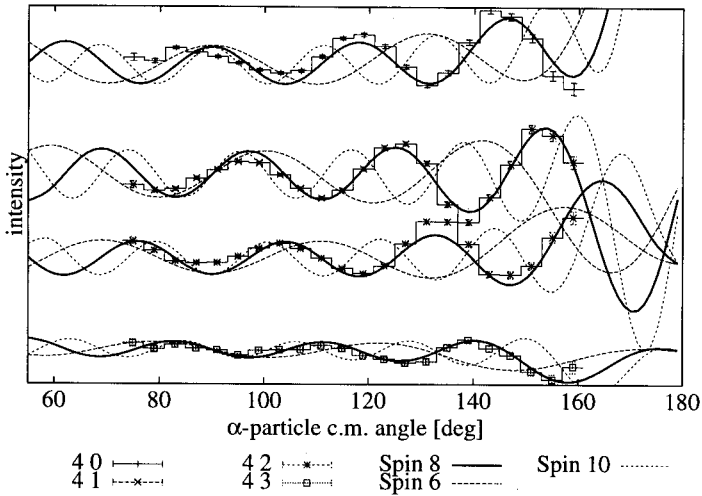


Figure 3. Sample triple angular correlation data observed for the  $\alpha_1\gamma$  decay of the 16.5 MeV state, analyzed with equation (6). Plotted from top to bottom are the correlation data for  $(\lambda_0 q_0) = (4, 0)(4, 1)(4, 2)(4, 3)$ , together with the distributions calculated for spin 8 (bold), 6 (dash), and 10 (dotted).

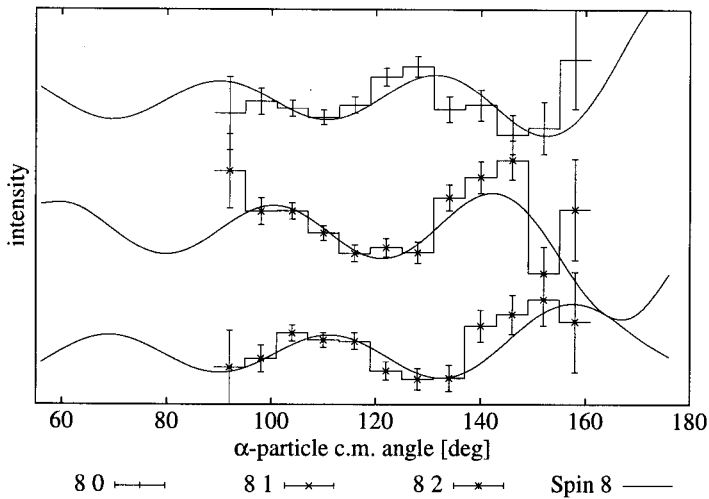


Figure 4. Sample quadruple angular correlation data observed for the  $\alpha_1\gamma\gamma$  decay of the 17.1 MeV state, analyzed with equation (7). Plotted from top to bottom are the correlation data for  $(\lambda_0 q_0) = (8, 0)(8, 1)(8, 2)$ , together with the distributions calculated for spin 8.

## 5. DATA ANALYSIS

Using equation (6), we analyzed the triple ( $\alpha_1\gamma$ ) correlations for  $^{24}\text{Mg}$  states that subsequently  $\alpha_1$ -decay to the  $2^+$  level in  $^{20}\text{Ne}$ . Figure 3 shows the angular correlations observed in the decay of the 16.5 MeV state. The experimental values are corrected for the geometrical acceptance of the  $\alpha$ -detectors. We compare the experiment with correlations calculated for different spin assumptions, spin  $8^+$ ,  $6^+$  and  $10^+$ . The experimental distributions match the calculated patterns for all relevant ( $\lambda_0q_0$ ) indices for the spin 8,  $L=6$  hypothesis. The period of the angular oscillations is characteristic for the  $L$ -value of the  $\alpha$  transition and does not fit the other spin assumptions.

The quadruple ( $\alpha_1\gamma\gamma$ ) correlations for states feeding the  $4^+$  level were analyzed using equation (7). In Figure 4 we display the quadruple correlations measured in the decay of the 17.2 MeV state. The structure of the distributions is very similar to the cases of  $2^+$  decay, with characteristic oscillations depending on the angular momentum of the  $\alpha$ -particle. In total, the spin of four states could be determined with this new method. These results will be discussed elsewhere [6].

## 6. CONCLUSION

We measured population and decay of high-lying states in  $^{24}\text{Mg}$  using  $\alpha$ -spectroscopy in conjunction with  $\gamma$ -rays detected by GAMMASPHERE. We developed a new analysis method based on a Fourier transformation which allows us to analyze the triple angular correlations in unsurpassed detail. Furthermore, we analyzed for the first time the quadruple angular correlations of  $\alpha\gamma\gamma$  cascades, which allow for spin determination of states which could not be reached in previous experiments. The formalism developed for our experiment can be applied to analyze high-fold angular correlations measured with  $4\pi$  detector arrays.

## REFERENCES

1. A.H. Lumpkin, G.R. Morgan, J.D. Fox, K.W. Kemper, Phys. Rev. Lett. 40 (1978) 104
2. A. Szanto de Toledo, T.M. Cornier, M.M. Coimbra, N. Carlie Filho, P.M. Swertka, N.G. Nicolis, Phys. Rev. C30, (1984) 1706
3. R.W. Zurmühle, D.P. Balamuth, L.K. Fifield and J.W. Noé, Phys. Rev. Lett. 29 (1972) 795
4. L.K. Fifield, R.W. Zurmühle and D.P. Balamuth, Phys. Rev. C 8 (1973) 2217
5. K.C. Young, R.W. Zurmühle, J.M. Lind, D.P. Balamuth Nucl. Phys. A 330 (1979) 477
6. I. Wiedenhöver et al., to be published.
7. I.Y. Lee, Nucl. Phys. A520 (1990) 641c
8. R.M. Steffen and K. Alder, in *The electromagnetic interaction in nuclear spectroscopy*, ed., W.D. Hamilton, (1975) North-Holland Publish., Amsterdam.
9. I. Wiedenhöver et al., Phys. Rev. C 58 (1999) 721
10. M. Freer, Nucl. Instr. Meth. Phys. Res. A383 (1996) 463